

New approach to prepare Pt-based hydrogen diffusion anodes tolerant to CO for polymer electrolyte membrane fuel cells

Francisco Alcaide*, Óscar Miguel, Hans-Jürgen Grande

Energy Department, CIDETEC, Centre for Electrochemical Technologies, Paseo Miramón 196, E20009 Donostia-San Sebastián, Spain

Available online 7 July 2006

Abstract

A new approach to prepare Pt-based hydrogen diffusion anodes for PEMFCs based on galvanostatic pulsed electrodeposition is demonstrated to be a reliable alternative to the conventional electrode preparation methods. The performance of the PtRu electrodeposited anodes depends on the electrodeposition parameters such as the peak current, on time, off time, and the total charge applied. The peak current density and the relaxation time are crucial in the control of electrode performance. Electrodes prepared using a cathodic peak current of 0.400 A cm^{-2} , a duty cycle of 5.66% and a charge density of 6 C cm^{-2} demonstrate high catalytic performance towards hydrogen oxidation.

© 2006 Elsevier B.V. All rights reserved.

Keywords: Platinum–ruthenium; CO tolerance; Pulse electrodeposition; PEMFC; Hydrogen oxidation

1. Introduction

Polymer electrolyte membrane fuel cells (PEMFCs) operating with high-purity hydrogen as fuel show good performance over a wide range of conditions. However, in a hydrogen-based economy, cheap hydrogen is required [1]. This hydrogen gas can be produced with the aid of the reforming of an organic fuel, like natural gas, methanol or a gasoline fraction. The reforming process leads to the production of a mixture of hydrogen, carbon dioxide, carbon monoxide and nitrogen, whose final composition depends on the starting chemical in the reforming process, *e.g.*, from the steam reforming of methanol the typical composition of reformat gas is 75% H_2 , 24% CO_2 and 1% CO [2–4].

The hydrogen diffusion electrodes with a platinum loading of $0.1\text{--}0.2 \text{ mg cm}^{-2}$ show good performance in PEMFCs operating with pure hydrogen [5], and maintain this performance when the hydrogen is poisoned by trace amounts of CO. Nevertheless, concentrations of 10 ppm of CO in the hydrogen gas decrease the voltage by 0.2–0.3 V at 0.8 A cm^{-2} and 80°C , and a content of 250 ppm of CO leads to a dramatic loss of voltage of 0.4 V at 0.8 A cm^{-2} and 80°C [6].

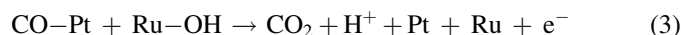
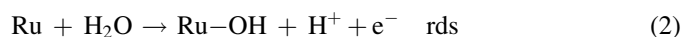
The common point of view with regard to the mechanism of the poisoning of platinum [7] is the blocking of sites available for the hydrogen adsorption by particles of CO, because the strength of the Pt–CO bond is higher when compared with the Pt–H bond. This hinders the dissociative adsorption of hydrogen on platinum and its subsequent ionization.

New binary, ternary and other catalytic systems, for example, Pt–M ($\text{M} = \text{Ru}, \text{Mo}, \text{W}, \text{Co}, \text{Ir}, \text{Ni}, \text{Sn}$), Pt/Ru–M ($\text{M} = \text{Au}, \text{Os}, \text{WO}_x, \text{SnO}_x$) [4,8–12], have been developed with the purpose of improving the tolerance of platinum with respect to poisoning by CO and to be equivalent to the performance displayed by platinum. The most reliable results concerning an increase in the tolerance to CO impurities in a hydrogen gas were obtained using ruthenium alloyed with platinum [13,14], as well as, nonalloyed bimetallic PtRu catalysts [15]. In fact, early studies in the 1960s already determined that PtRu catalysts show a significantly enhanced CO tolerance over Pt [16], but the use of PtRu catalysts for PEMFCs was not first proposed until the 1980s [17].

One explanation for the enhanced electrocatalytic activity of PtRu is related to the changes in the lattice structure and surface properties due to the alloying, which decrease the strength of the CO adsorption without increasing the overpotential for the hydrogen electrooxidation [18]; another is that the Ru in the electrocatalyst is in a partially oxidized state and provides the radical for the oxidative removal of CO adsorbed on neighboring platinum sites [19,20]. In fact, ruthenium has

* Corresponding author. Tel.: +34 943 309 022; fax: +34 943 309 136.
E-mail address: falcaide@cidetec.es (F. Alcaide).

the ability to form OH_{ads} from water at significantly lower potentials than platinum. The mechanism of the electrooxidation of CO adsorbed on platinum can be summarized as follows:



where in Eq. (2) rds denotes rate determining step of the process.

The influence of the Pt:Ru ratio on CO tolerance has been studied extensively [21]. Despite certain results related to the variation of Pt:Ru atomic ratio with the CO concentration [20,22,23], it seems that the optimum atomic ratio between Pt and Ru is 50:50 [2,24,25].

Nowadays, a large-scale commercialization of the PEMFC technology requires a further reduction of the amount of catalyst in membrane/electrodes assemblies (MEAs) [26]. In fact, gas diffusion electrodes made with conventional methods, which use powder catalysts, contain catalyst layers with inactive catalytic sites [27]. This low catalyst utilisation can be avoided using a method that allows the catalyst to be localized only where the electrochemical reaction takes place.

Electrodeposition methods in aqueous solution permit the distribution of catalyst selectively on the surface of the electrode, specifically, at the membrane–electrode interface. In this way it is possible to improve catalyst utilisation and to decrease its loading (and cost) in electrodes and MEAs. In fact, constant and pulsed potential and current techniques have been applied to catalyse electrodes with Pt and PtRu with the aim to prepare MEAs for H_2/O_2 PEMFCs [28,29] and liquid direct methanol fuel cells, DMFCs [30], and to study oxygen reduction and methanol oxidation reactions [31–36], but, until now, no attempts has been made to use PtRu catalysed electrodes as hydrogen anodes tolerant to CO.

The objective of the present work is to use galvanostatic pulse electrodeposition as an electrochemical technique to prepare catalytic PtRu electrodeposited hydrogen diffusion anodes. We also study the effect of the electrodeposition parameters on the electrodes tolerance to CO and their performance towards the anodic hydrogen oxidation reaction.

2. Experimental

Solutions were prepared with ultrapure water, with conductivity less than $5.4 \times 10^{-8} \Omega^{-1} \text{cm}^{-1}$, obtained from a Millipore-Milli-Q system. Isopropyl alcohol, ethanol, polytetrafluoroethylene aqueous suspension and Nafion[®] dispersion (Aldrich[®]) were used as received. $\text{H}_2\text{PtCl}_6 \cdot 6\text{H}_2\text{O}$, K_2RuCl_5 (Alfa Aesar[®]) and H_2SO_4 (Merck[®]) were RG quality products. High-purity gases: N_2 (99.999%), 1000 ppm CO/ N_2 (99.95%) and 10 ppm CO/ H_2 (99.999%) from Praxair Inc. were used in the experiments.

The non-catalysed electrodes were composed of a Nafion[®] bonded carbon support sprayed onto a gas diffusion layer. The gas diffusion layer was prepared by mixing appropriate amounts

of Vulcan XC-72 (Cabot Corp.) and polytetrafluoroethylene aqueous suspension (60 wt.%) with isopropyl alcohol, and then applying the paste into a hydrophobic carbon cloth (type A, from E-Tek, Inc.). Finally, the hydrophobic layer was sintered at 350 °C for 0.5 h in air to remove organic solvents. An ink made with Vulcan XC-72, Nafion[®] dispersion (5 wt.%), isopropyl alcohol and ultrapure water, under ultrasonic agitation, was applied on the hydrophobic carbon layer at a loading of 2.0 mg cm^{-2} . The weight per square centimeter of the non-catalysed electrodes including the cloth was about 23 mg.

The electrochemical catalysation with Pt or PtRu was performed in a two-electrode glass cell. The cell was divided by a proton exchange membrane to avoid the formation of undesirable products on the platinum mesh, which served as counter electrode. The working electrode was a circular piece of a non-catalysed electrode, mounted into a holder that provided an exposed area to the solution of 0.79 cm^2 . The rear side of the working electrode was in electrical contact with a gold plate current collector. K_2RuCl_5 and/or H_2PtCl_6 5.0 mmol dm^{-3} equimolar solutions in aqueous H_2SO_4 1.0 mol dm^{-3} and pure H_2SO_4 1.0 mol dm^{-3} were used as electrolyte in the working and counter electrode compartments of the cell, respectively. Then, rectangular galvanostatic pulses at different peak current densities and duty cycles were applied to deposit Pt and PtRu on working electrodes, under N_2 inert atmosphere at room temperature. In all cases, the total amount of charge density was fixed at 6 C cm^{-2} .

Once the electrode was catalysed, it was washed in stirred hot ultrapure water for several hours, primarily to remove the chloride ions. After that, the electrode was sprayed with an ethanolic Nafion[®] dispersion and then dried at 130 °C for 2 h under vacuum conditions. The ionomer loading of the electrode was 0.8 mg cm^{-2} .

Scanning electron microscopy (SEM) observations were carried out using a JSM5910-LV JEOL microscope. The EDX measurements were performed with an INCA-300 energy analyser.

Electrochemical measurements were performed with a potentiostat/galvanostat PGSTAT 30 (Eco Chemie) driven by the GPES software in a three-electrode two compartments thermostated glass cell. Measured currents were normalized using the geometric electrode area, unless otherwise stated. The working electrode was a Pt or PtRu catalysed electrode located inside a cylindrical holder, which had an inlet and an outlet that allowed the circulation of gases. The geometrical area exposed to the solution was 0.79 cm^2 . The counter electrode was a platinum wire or sheet, which was introduced in a compartment separated from the main solution by a glass frit. The reference electrode was $\text{Hg}_2\text{SO}_4|\text{Hg}$, K_2SO_4 sat (MSE) immersed in a glass tube connected with the main compartment of the cell via a Luggin–Haber capillary, situated close to the working electrode surface, but all the electrode potentials throughout this paper will be referred to the RHE scale. The electrolyte was a 0.5 mol dm^{-3} H_2SO_4 aqueous solution, deaerated by bubbling N_2 .

Cyclic voltammograms were recorded in N_2 atmosphere at a scan rate of 20 mV s^{-1} until reproducible voltammograms were obtained at 25.0 °C.

CO voltammetric stripping experiments were performed feeding the working electrode with a mixture of 0.1% CO in N₂ at 0.250 cm³ min⁻¹ at atmospheric pressure for 50 min, while holding the electrode potential at 0.100 V vs. RHE (−0.605 V vs. MSE). After the adsorption, the CO was removed from the solution by N₂ bubbling and the electrode gas feed was switched to N₂ for 20 min, while still holding the admission potential, to remove any CO from the holder. Then, two CO stripping voltammograms were recorded in the positive direction at 20 mV s⁻¹.

The electrocatalytic activity of the PtRu catalysed electrodes against the hydrogen oxidation was evaluated at 60 °C by linear sweep voltammetry measurements registered at a scan rate of 1 mV s⁻¹. The working electrode was fed with prehumidified 10 ppm CO/H₂ mixture at 100 cm³ min⁻¹, while N₂ was passed over the solution. The humidification temperature was 15 °C higher than the cell temperature. Ohmic drop in solution was not corrected.

3. Results and discussion

3.1. Effect of galvanostatic pulse electrodeposition operating conditions on CO oxidation for PtRu and Pt catalysed electrodes

In this work, galvanostatic pulse deposition consists of the application of a periodic cathodic current density, j_p , during the on time, t_{on} , and switching off the current during the off time, t_{off} . The average current density, j_a , is defined as $j_p[t_{on}/(t_{on} + t_{off})]$, where the duty cycle, γ , is the expression between brackets multiplied by 100. Pulse electrodeposition thus has three independent variables, namely, the peak current density, j_p , the on time, t_{on} , and the off time, t_{off} . Two main approaches are generally used: varying j_p with constant t_{on} and j_a , or varying j_p with constant $j_a(t_{on} + t_{off})$. Since both j_p and t_{off} influence crystallization (nucleation and growth) [37], we have used the second technique, where the off time does not vary very much. The catalyst loading in the electrode is controlled by the total charge density applied. Several electrodes were catalysed with PtRu by galvanostatic pulse deposition, using the experimental conditions listed in Table 1. The total current passed was 4.74 C. In general, the reported current efficiency of this electrodeposition process is around 10% [30,35].

Table 1
Electrodeposition parameters used in the catalysation of the electrodes with PtRu

j_p^a (A cm ⁻²)	t_{on} (s)	t_{off} (s)	γ^b (%)	Pt:Ru ^c (%)
0.050	0.024	0.079	23.30	50.3:49.7
0.100	0.012	0.091	11.65	52.9:47.1
0.200	0.006	0.097	5.82	52.4:47.6
0.400	0.003	0.050	5.66	48.5:51.5
0.400	0.003	0.100	2.91	49.9:50.1
0.400	0.003	0.200	1.48	51.9:48.1

^a Values normalized to the geometric area of the electrode.

^b Duty cycle.

^c Pt:Ru atomic ratio.

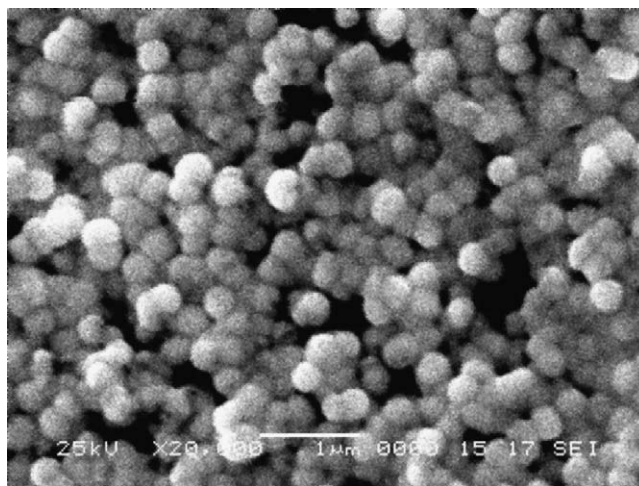


Fig. 1. SEM micrograph of a 50:50 PtRu catalysed electrode prepared by galvanostatic pulse electrodeposition at j_p 0.050 A cm⁻² and a duty cycle 23.3%.

Fig. 1 shows a typical scanning electron micrograph of the surface of a PtRu electrode fabricated by galvanostatic pulse electrodeposition. We have confirmed that the nucleation and growth of crystals are influenced manifestly by the surface state of the Nafion[®] bonded carbon support. A granular deposit of particles with an average diameter of 0.35 μm covers the support's surface. In addition, no dendritic growth of the deposit, expected when the concentration polarization is large, is observed.

Table 1 shows the atomic composition of the catalysed surfaces of the electrodes prepared in this work determined by EDX. The PtRu compositions detailed here represent the average of four different measurements on the same electrode. These values presented a standard relative error less than 1%. Between electrodes prepared with the same set of parameters (j_p , t_{on} , t_{off}) the standard relative error is 1–2%. In general, the PtRu atomic ratio experimental values obtained are close the 50:50 PtRu atomic ratio in solution. Moreover, the emitted radiation energies are $L_{\alpha} = 9.441$ kV and $M = 2.048$ kV for Pt and $L_{\alpha} = 2.558$ kV and $M = 0.461$ kV for Ru. The closeness of the L energy for Ru and the value of the M radiation for Pt, may introduce errors. In addition, because of the penetration depth of this analysis, it provides bulk compositions, which do not necessarily correspond to the surface composition.

Cyclic voltammograms in inert atmosphere for the electrodes listed in Table 1 are shown in Fig. 2. In contrast to the well-known cyclic voltammogram of polycrystalline platinum [38], the characteristic adsorption/desorption hydrogen peaks are not observed, because the formation of ruthenium oxides at those potentials [39]. In fact, the cyclic voltammograms of PtRu catalysed electrodes are dominated by Ru-like structures and their shapes are in agreement with the relative Pt:Ru ratio [40]. The broad capacitive features found in the curves of Fig. 2 are characteristic of a RuO_xH_y phase [41].

Fig. 3 shows the cyclic voltammograms for the oxidation of CO on the most representative PtRu catalysed electrodes of Table 1 and their respective backgrounds.

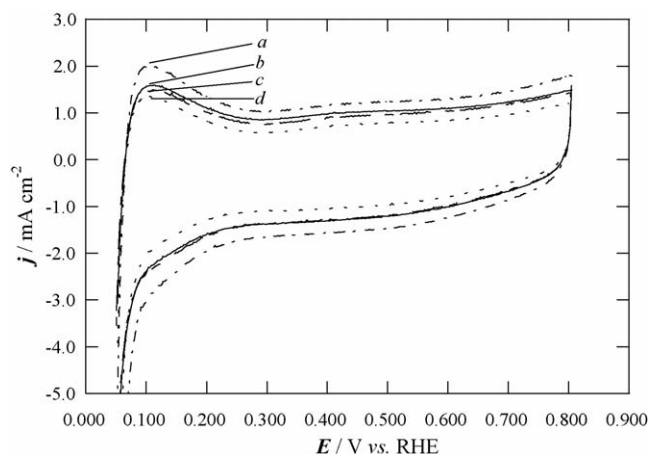


Fig. 2. Cyclic voltammograms of the PtRu electrodes prepared by pulse electrodeposition: (a) j_p 0.400 A cm^{-2} , γ 2.91%; (b) j_p 0.050 A cm^{-2} , γ 23.3%; (c) j_p 0.100 A cm^{-2} , γ 11.65%; (d) j_p 0.200 A cm^{-2} , γ 5.82%, in inert N_2 atmosphere and H_2SO_4 0.50 mol dm^{-3} , $v_s = 20 \text{ mV s}^{-1}$, $T = 25.0^\circ\text{C}$.

The characteristics of CO stripping voltammograms were essentially the same for each set of PtRu electrodes analysed. The hydrogen oxidation current at the beginning of the scan is suppressed due to its displacement by the adsorbed CO. The first scan reveals a maximum where the adsorbed CO is oxidized. The second scan practically fits with voltammetric curves measured in the supporting solution deaerated with N_2 . That means that the adsorbed monolayer of CO was fully oxidized during the first scan. On the other hand, the fact that the electric double layer charging current on the second scan after the CO oxidation is slightly higher than that of the first scan, can be attributed to the pseudocapacitance of the PtRu metal within the inner-Helmholtz plane [42].

The CO oxidation peak is a more or less sharp peak whose peak potential and width depends on the surface electrode composition. In Fig. 3, the onset of oxidation of the CO adlayer starts at about 0.400 V and broad stripping current peaks are

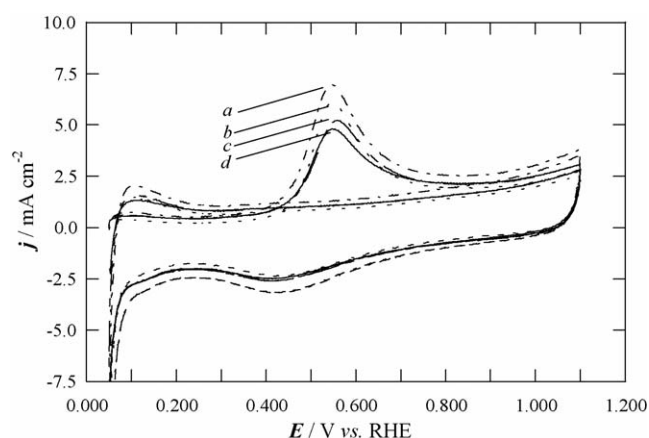
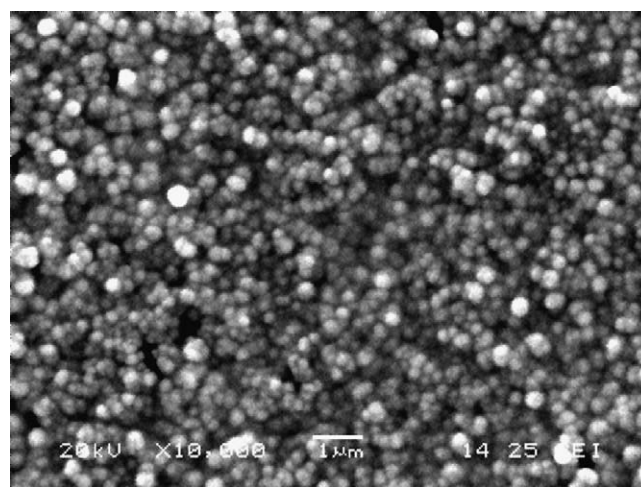


Fig. 3. CO stripping voltammograms of the PtRu electrodeposited electrodes prepared by pulse electrodeposition: (a) j_p 0.400 A cm^{-2} , γ 2.91%; (b) j_p 0.200 A cm^{-2} , γ 12.8%; (c) j_p 0.100 A cm^{-2} , γ 11.65%; (d) j_p 0.050 A cm^{-2} , γ 23.3%, in N_2 inert atmosphere 0.5 mol dm^{-3} aqueous solution H_2SO_4 at 25.0°C , $v_s = 20 \text{ mV s}^{-1}$. The second scans after the CO_{ads} monolayer oxidation are also included. CO was adsorbed at 0.1 V vs. RHE for 40 min.

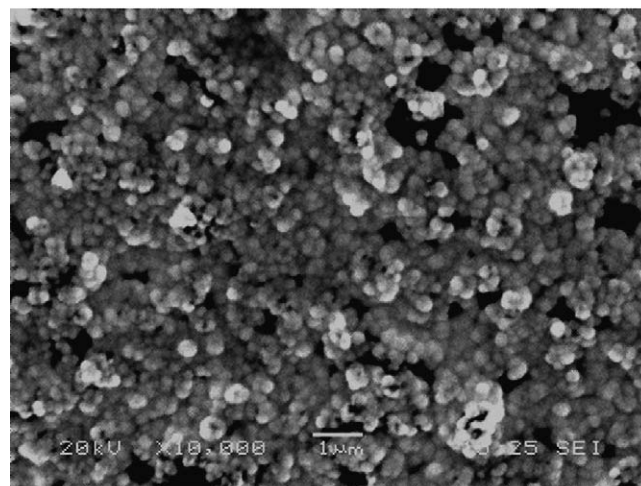
seen between 0.546 and 0.560 V, within the experimental error ($\pm 10 \text{ mV}$). These values as well as the peak shape are consistent with those reported in the literature [42–44].

The rate determining step of galvanostatic pulse electrodeposition is controlled by mass transport [45]. As such, several electrodes were catalysed varying the off time (see Table 1) to study the effect of re-equilibrating the concentration of Pt and Ru complexes at the electrodes surfaces on their physical characteristics. CO stripping voltammograms (not shown) have similar features previously found in Fig. 3. The CO oxidation peaks of the electrodes catalysed at 50 and 200 ms off time are in the range of 0.534–0.539 and 0.549–0.559 V, respectively, within the experimental error. As shown in Fig. 4, it seems that a decrease in the off time causes a reduction in the grain size of the deposit. A similar behavior has been reported regarding the methanol oxidation reaction [30].

Fig. 5 shows the CO stripping voltammograms corresponding to Pt and PtRu catalysed electrodes prepared following the same conditions. The CO oxidation peak potential of the Pt electrodeposited electrode is 0.724 V. This value that can



(a)



(b)

Fig. 4. SEM micrographs of PtRu catalysed electrodes prepared by galvanostatic pulse electrodeposition with different duty cycles: (a) 5.66%; (b) 2.91%.

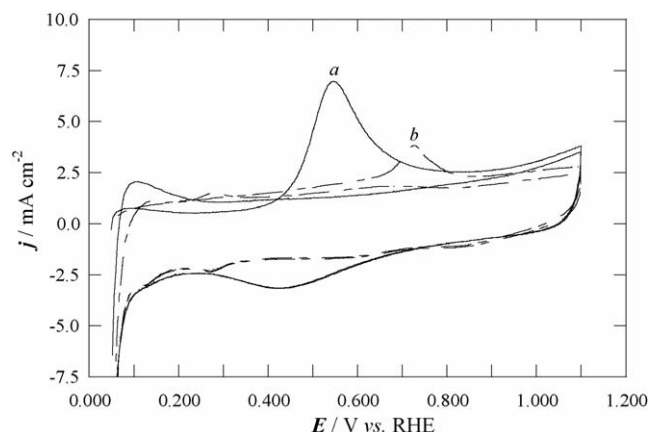


Fig. 5. CO stripping voltammograms and second scans of (a) PtRu and (b) Pt electrodeposited electrodes prepared by pulse electrodeposition at j_p 0.400 A cm^{-2} and γ 2.91%, in the same conditions as in Fig. 3.

depend on several factors agrees with those found in the literature [46–48]. The second scan allows seeing the characteristics hydrogen adsorption/desorption peaks of polycrystalline platinum. On the other hand, the onset of the CO oxidation current of the PtRu electrodeposited electrode starts at 0.350 V, a considerably more negative potential than for CO on Pt. In the same way, the CO stripping peak in PtRu is shifted around 0.200 V negative compared to that for Pt, in agreement with the reported data [43]. This means that the apparent electrocatalytic activity of the PtRu electrodeposited electrode is superior to that of the Pt electrode.

For assessing the catalytic activity of the different PtRu electrodeposited electrodes, however, the measured currents should be normalized with respect to their electrochemically active surface area. Table 2 summarizes the electrochemically active surface areas of the PtRu catalysts estimated from the charge associated to the CO_{ads} stripping peak (corrected for the effects of double layer charging currents and oxide growth), and assuming that one monolayer of adsorbed CO linearly bonded requires $420 \mu\text{C cm}^{-2}$ for its oxidation [49,50].

From Table 2, one can observe that peak current density, j_p , affects the electrochemically active surface, EAS, of the PtRu catalysts. In fact, an increase in j_p , leads to a high EAS. This behavior could be explained by taking into account that in an electrochemical deposition: $r_c \propto 1/|\eta|$, where r_c is the critical

radius of nucleation (particles with $r > r_c$ are stable), and η is the overpotential [51]. Thus, the higher the current density applied, the higher the overpotential, and the smaller the particle size. Therefore, a high active surface area would be expected.

The roughness factor, R_f , describes the enhancement of real electrode surface area in comparison with a smooth surface. It can be defined as $R_f = \text{EAS}/A_g$, where EAS is the real electrochemically active surface area, in $\text{cm}^2 \text{ PtRu}$, and A_g is the geometric electrode area, 0.79 cm^2 in the present work. Table 2 shows roughness factors of PtRu catalysed electrodes calculated from the EAS values. On the other hand, if we consider, as first approximation, that catalyst particles are spherical and non-porous, theoretically roughness factor can be calculated from the following formula: $R_f = SW$, where S is the specific surface area, in $\text{cm}^2 \text{ g}^{-1}$ of catalyst, and W is the catalyst loading, in gram of catalyst per square centimeter [18,52].

It is worth comparing the roughness factors of PtRu electrodeposited electrodes with those typically achieved in conventional PtRu catalysed electrodes employed in PEMFCs. Such hydrogen diffusion anodes, usually fabricated following thin-film methods [53], contain carbon supported PtRu catalysts in their active layers to improve their tolerance towards CO impurities present in fuel stream. Catalyst loading is varied according to the composition of the fuel inlet, in order to optimize their performance. In this sense, Gasteiger et al. stated that $0.2 \text{ mg PtRu cm}^{-2}$ was the minimum catalyst loading necessary for reformat containing 100 ppm CO operation with a 2% air-bleed, using state-of-the-art PtRu catalysts [54]. For example, one can consider the use of a catalyst 20 wt.% Pt–10 wt.% Ru (1:1 at. ratio)/Vulcan XC-72 (Johnson Matthey), which has a specific surface area of $58 \text{ m}^2 \text{ g}^{-1} \text{ PtRu}$ [12]. This translates to a R_f value in the range of $348\text{--}116 \text{ cm}^2 \text{ PtRu cm}^{-2}$ at catalyst loadings of 0.6 and $0.2 \text{ mg PtRu cm}^{-2}$, respectively. The potentially available PtRu surface area is roughly the same in electrodeposited PtRu j_p 0.400 A cm^{-2} and γ 2.91% electrode at a loading of $0.12 \text{ mg PtRu cm}^{-2}$, as one can see in Table 2.

3.2. Electrooxidation of 10 ppm CO/H_2 mixture with the Pt–Ru electrodeposited electrodes

The anodic oxidation of H_2/CO mixture on PtRu catalysed electrodes was investigated by linear sweep voltammetry. The concentration of CO was 10 ppm, following the requirements of practical systems, because at this concentration the PtRu anode is not severely poisoned. Curves shown in Figs. 6 and 7, in which currents have been normalized by EAS values from Table 2, are representative for each set of electrodes, within the experimental error ($\sim 5\%$).

Fig. 6 shows the quasi-stationary $j_{\text{an}}\text{--}E$ curves for hydrogen oxidation on the PtRu electrodes of Fig. 3. The very high slopes observed for each electrode, as well as the limiting current densities attained indicates that the reaction is controlled by mass transfer. In fact, the hydrogen oxidation reaction is so fast reaction that it becomes very difficult to determine its

Table 2
Electrochemically active surface areas, EAS, estimation from CO stripping cyclic voltammetries

j_p (A cm^{-2})	γ^a (%)	Q_{ox}^b (C)	EAS (cm^2)	R_f^c ($\text{cm}^2 \text{ PtRu}$) (cm^{-2})
0.050	23.30	0.0255	60.7	77
0.100	11.65	0.0278	66.1	84
0.200	5.82	0.0301	71.7	91
0.400	5.66	0.0214	50.1	63
0.400	2.91	0.0336	80.0	101
0.400	1.48	0.0308	73.3	93

^a Duty cycle.

^b CO oxidation charge.

^c Roughness factor (see text).

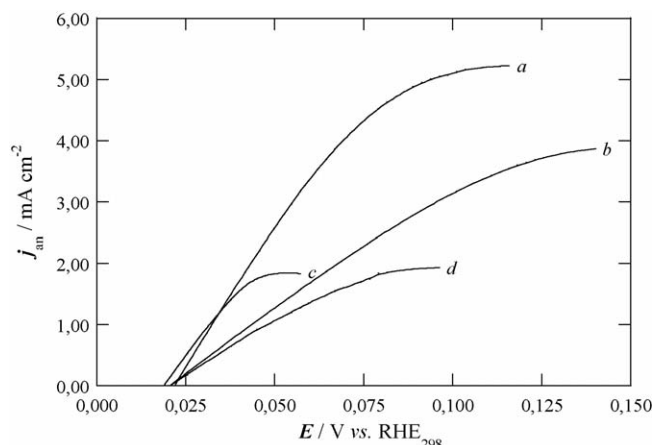


Fig. 6. $j_{\text{an}}-E$ curves of the anodic oxidation of 10 ppm CO/H_2 on PtRu electrodeposited electrodes in $0.5 \text{ mol dm}^{-3} \text{ H}_2\text{SO}_4$: (a) j_p 0.400 A cm^{-2} , γ 2.91%; (b) j_p 0.200 A cm^{-2} , γ 5.82%; (c) j_p 0.050 A cm^{-2} , γ 23.3%; (d) j_p 0.100 A cm^{-2} , γ 11.65%. Temperature 60.0°C . $v_s = 1 \text{ mV s}^{-1}$. The fully humidified gas was fed at 100 ml min^{-1} . Atmospheric pressure.

electrochemical parameters, e.g., exchange current density and tafel slope, due to the interference from mass transport resistances. Nevertheless, it seems that its rate determining step may be H_2 dissociation [55,56]. From Fig. 6, the electrode catalysed at j_p 0.400 A cm^{-2} and γ 2.91% displays the best performance. This electrode showed a geometric current density of 0.34 A cm^{-2} at 0.075 V .

The quasi-stationary $j_{\text{an}}-E$ curves reported in Fig. 7, are those in which the duty cycle was varied. The best performance against hydrogen oxidation is shown for the electrode prepared at j_p 0.400 A cm^{-2} and a duty cycle of 5.66%. This electrode showed a geometric current density of 0.39 A cm^{-2} at 0.075 V . This behavior could be attributed to the fact that catalytic activity of PtRu electrodes depends also on the different surface distribution of atoms at the electrode surface. In addition, higher electrocatalyst surface areas are not directly related to

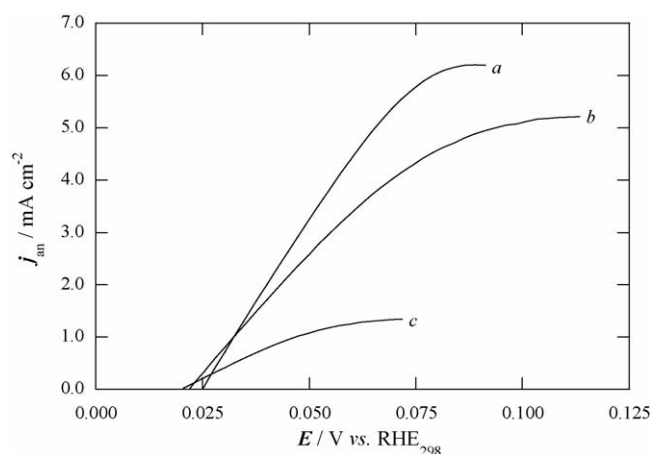


Fig. 7. $j_{\text{an}}-E$ curves of the anodic oxidation of 10 ppm CO/H_2 on PtRu electrodeposited electrodes in $0.5 \text{ mol dm}^{-3} \text{ H}_2\text{SO}_4$. Effect of duty cycle, γ : (a) 5.66% and (c) 1.48%. The j_p was 0.400 A cm^{-2} . Temperature 60.0°C . $v_s = 1 \text{ mV s}^{-1}$. The fully humidified gas was fed at 100 ml min^{-1} . Atmospheric pressure.

higher performance as a result of kinetic, ohmic and mass transport losses within the electrode matrix. Nevertheless, further studies are required on this issue.

4. Conclusions

In this work we have shown that galvanostatic pulse electrodeposition is a reliable technique to prepare PtRu catalysed hydrogen diffusion anodes tolerant to CO. The PtRu is localized on the surface of carbon support electrode. In this way, it is possible to decrease the thickness of the catalyst layer and increase the catalyst utilisation. Moreover, the catalyst loading and the composition (atomic ratio) of the electrodes are also controllable. The electrodes performance towards the anodic hydrogen oxidation depends on the electrodeposition parameters: by increasing the peak current density, j_p , the catalytic activity of the electrodes is increased. In addition, a longer deposition time, t_{off} , reduces the electrodes catalytic activity. Prior to the preparation of MEAs, further studies are also necessary to establish the influence of the electrodeposition parameters on the structure of catalysts, as well as to assess the current efficiency of the process in detail.

Acknowledgements

The authors gratefully acknowledge the financial support of this work provided by the Ministry of Industry of the Spanish Government (PROFIT-support for technological centres G20588588/05), the Diputación Foral de Gipuzkoa, the Basque Country Government (ETORTEK program) and CEGASA.

References

- [1] T. Rostrup-Nielsen, Catal. Today 106 (2005) 293.
- [2] F. Joensen, J.R. Rostrup-Nielsen, J. Power Sources 105 (2002) 195.
- [3] B. Höhle, M. Boe, J. Bøggild-Hansen, P. Bröckerhoff, G. Colsman, B. Emonts, R. Menzer, E. Riedel, J. Power Sources 61 (1996) 143.
- [4] A.T. Haug, R.E. White, J.W. Weidner, W. Huang, J. Electrochem. Soc. 149 (2002) A862.
- [5] H. Kim, J.-N. Park, W.-H. Lee, Catal. Today 87 (2003) 237.
- [6] H.-F. Oetjen, V.M. Schmidt, U. Stimming, F.J. Trila, J. Electrochem. Soc. 143 (1993) 3838.
- [7] B.E. Conway, B.V. Tilak, Electrochim. Acta 47 (2002) 3571.
- [8] V. Mehta, J.S. Cooper, J. Power Sources 114 (2003) 32.
- [9] W.C. Choi, M.K. Jeon, Y.J. Kim, S.I. Woo, W.H. Hong, Catal. Today 93–95 (2004) 517.
- [10] M.S. Chen, D.W. Goodman, Catal. Today 111 (2006) 22.
- [11] J. Greeley, M. Mavrikakis, Catal. Today 111 (2006) 52.
- [12] C. He, H.R. Kunz, J.M. Fenton, J. Electrochem. Soc. 150 (2003) A1017.
- [13] H.A. Gasteiger, N.M. Marcovic, P.N. Ross, E.J. Cairns, J. Phys. Chem. 98 (1994) 617.
- [14] Y.J. Zhang, A. Maroto-Valiente, I. Rodriguez-Ramos, Q. Xin, A. Guerrero-Ruiz, Catal. Today 93–95 (2004) 619.
- [15] K.A. Friedrich, K.P. Geyzers, A.J. Dickinson, U. Stimming, J. Electroanal. Chem. 524–525 (2002) 261.
- [16] L.W. Niedrach, D.W. McKee, J. Paynter, I.F. Danzig, Electrochem. Technol. 5 (1967) 318.
- [17] G.A. Eisman, in: J.W. Van Zee, R.E. White, K. Kinoshita, H.S. Burney (Eds.), Proceedings of the Symposium on Diaphragms, Separators and Ion-exchange Membranes, PV 86-13, The Electrochemical Society Proceedings Series, Pennington, NJ, (1986), p. 156.

- [18] L. Giorgi, A. Pozio, C. Bracchini, R. Giorgi, S. Turtu, *J. Appl. Electrochem.* 31 (2001) 325.
- [19] K.A. Friedrich, K.P. Geyzers, U. Linke, U. Stimming, J. Stumper, *J. Electroanal. Chem.* 402 (1996) 123.
- [20] H.A. Gasteiger, N.M. Marković, P.N. Ross, *J. Phys. Chem.* 99 (1995) 16757.
- [21] K. Ruth, M. Vogt, R. Zuber, in: W. Vielstich, H.A. Gasteiger, A. Lamm (Eds.), *Handbook of Fuel Cells—Fundamentals, Technology and Applications*, vol. 3, John Wiley & Sons, Ltd., Chichester, UK, 2003, p. 489.
- [22] M. Iwase, S. Kawatsu, in: S. Gottesfeld, G. Halpert, A. Landgrebe (Eds.), *Proceedings of the First International Symposium on Proton Conducting Membrane Fuel cells*, PV 95-23, The Electrochemical Society Proceedings Series, Pennington, NJ, (1995), p. 12.
- [23] T. Tada, M. Inque, Y. Yamamoto, European Patent 1,022,795 (2000).
- [24] Z. Qi, A. Kaufman, *J. Power Sources* 113 (2003) 115.
- [25] A. Hammet, *Catal. Today* 38 (1997) 445.
- [26] H.A. Gasteiger, J.E. Panels, S.G. Yan, *J. Power Sources* 127 (2004) 162.
- [27] L. Guangchun, P.G. Pickup, *J. Electrochem. Soc.* 150 (2003) C745.
- [28] K.H. Choi, H.S. Kim, T.H. Lee, *J. Power Sources* 75 (1998) 230.
- [29] H. Kim, N.P. Subremanian, B.N. Popov, *J. Power Sources* 138 (2004) 14.
- [30] C. Countanceau, A.F. Rakotonrainibé, A. Lima, E. Garnier, S. Pronier, J.-M. Léger, C. Lamy, *J. Appl. Electrochem.* 34 (2004) 61.
- [31] E.J. Taylor, E.B. Anderson, N.R.K. Vilambi, *J. Electrochem. Soc.* 139 (1992) L45.
- [32] M.P. Hogarth, J. Munk, A.K. Shukla, A. Hammet, *J. Appl. Electrochem.* 24 (1994) 85.
- [33] F. Gloaguen, J.-M. Léger, C. Lamy, *J. Appl. Electrochem.* 27 (1997) 1052.
- [34] M.-S. Löffler, B. GroB, H. Natter, R. Hempelmann, Th. Krajewski, J. Divisek, *Phys. Chem. Chem. Phys.* 3 (2001) 333.
- [35] Z.D. Wei, S.H. Chan, *J. Electroanal. Chem.* 569 (2004) 23.
- [36] A. Missiroli, F. Soavi, M. Mastragostino, *Electrochem. Solid-State Lett.* 8 (2005) A110.
- [37] J.C. Puipe, F. Leeman (Eds.), *Theory and Practice of Pulse Plating*, American Electroplating and Surface Finishing Society, Orlando, 1986.
- [38] H. Angerstein-Kozłowska, in: E. Yeager, J.O'M. Bockris, B.E. Conway, S. Sarangapani (Eds.), *Comprehensive Treatise of Electrochemistry*, vol. 9, Plenum Press, New York, 1984, p. 15.
- [39] E.A. Ticianelli, J.G. Beery, M.T. Paffet, S. Gottesfeld, *J. Electroanal. Chem.* 258 (1989) 61.
- [40] F. Richarz, B. Wohlmann, U. Vogel, H. Hoffschulz, K. Wandelt, *Surf. Sci.* 335 (1995) 361.
- [41] J.W. Long, R.M. Stroud, K.E. Swider-Lyons, D.R. Rolison, *J. Phys. Chem. B* 104 (2000) 9772.
- [42] T. Kawaguchi, W. Sugimoto, Y. Murakami, Y. Takasu, *Electrochem. Commun.* 6 (2004) 480.
- [43] Z. Jusys, T.J. Schmidt, L. Dubau, K. Lasch, L. Jörissen, J. Garche, R.J. Behm, *J. Power Sources* 105 (2002) 297.
- [44] F. Colmati, W.H. Lizcano-Valbuena, G.A. Camara, E.A. Ticianelli, E.R. González, *J. Braz. Chem. Soc.* 13 (2002) 474.
- [45] H.Y. Cheh, *J. Electrochem. Soc.* 118 (1971) 1132.
- [46] H.A. Gasteiger, N.M. Markovic, P.N. Ross, *J. Phys. Chem.* 99 (1995) 8290.
- [47] J.P. Iúdice de Souza, T. Iwasita, F.C. Nart, W. Vielstich, *J. Appl. Electrochem.* 30 (2000) 43.
- [48] Z. Jusys, J. Kaiser, R.J. Behm, *Phys. Chem. Chem. Phys.* 3 (2001) 4650.
- [49] W.F. Lin, T. Iwasita, W. Vielstich, *J. Phys. Chem. B* 103 (1999) 3250.
- [50] K. Kinoshita, P.N. Ross, *J. Electroanal. Chem.* 78 (1977) 313.
- [51] E. Budevski, G. Staikov, W. Lorenz, *Electrochemical Phase Transformation and Growth*, VCH, Weinheim, 1996.
- [52] L. Spennadel, M. Boudart, *J. Phys. Chem.* 64 (1960) 204.
- [53] S. Litster, G. McLean, *J. Power Sources* 130 (2004) 61.
- [54] H.A. Gasteiger, J.E. Panels, S.G. Yan, *J. Power Sources* 127 (2004) 162.
- [55] R.J. Belows, E. Marucchi-Soos, in: S. Gottesfeld, T.F. Fuller, G. Halper (Eds.), *Proton Conducting Membrane Fuel cells*, PV 98-27, The Electrochemical Society Proceedings Series, Pennington, NJ, (1998), p. 218.
- [56] N.M. Markovic, B.N. Grgur, P.N. Ross, *J. Phys. Chem. B* 101 (1997) 5405.